

Effects of Deletion of ER α in Osteoblast-Lineage Cells on Bone Mass and Adaptation to Mechanical Loading Differ in Female and Male Mice

Katherine M Melville,^{1,2} Natalie H Kelly,^{1,2} Gina Surita,³ Daniel B Buchalter,³ John C Schimenti,⁴ Russell P Main,^{5,6} F Patrick Ross,⁷ and Marjolein CH van der Meulen^{1,2,7}

¹Sibley School of Mechanical and Aerospace Engineering, Cornell University, Ithaca, NY, USA

²Department of Biomedical Engineering, Cornell University, Ithaca, NY, USA

³Department of Biological Sciences, Cornell University, Ithaca, NY, USA

⁴College of Veterinary Medicine, Cornell University, Ithaca, NY, USA

⁵College of Veterinary Medicine, Purdue University, West Lafayette, IN, USA

⁶Weldon School of Biomedical Engineering, Purdue University, West Lafayette, IN, USA

⁷Research Division, Hospital for Special Surgery, New York, NY, USA

ABSTRACT

Estrogen receptor alpha (ER α) has been implicated in bone's response to mechanical loading in both males and females. ER α in osteoblast lineage cells is important for determining bone mass, but results depend on animal sex and the cellular stage at which ER α is deleted. We demonstrated previously that when ER α is deleted from mature osteoblasts and osteocytes in mixed-background female mice, bone mass and strength are decreased. However, few studies exist examining the skeletal response to loading in bone cell-specific ER α KO mice. Therefore, we crossed ER α floxed ($ER\alpha^{fl/fl}$) and osteocalcin-Cre (OC-Cre) mice to generate animals lacking ER α in mature osteoblasts and osteocytes (pOC-ER α KO) and littermate controls (LC). At 10 weeks of age, the left tibia was loaded in vivo for 2 weeks. We analyzed bone mass through micro-CT, bone formation rate by dynamic histomorphometry, bone strength from mechanical testing, and osteoblast and osteoclast activity by serum chemistry and immunohistochemistry. ER α in mature osteoblasts differentially regulated bone mass in males and females. Compared with LC, female pOC-ER α KO mice had decreased cortical and cancellous bone mass, whereas male pOC-ER α KO mice had equal or greater bone mass than LC. Bone mass results correlated with decreased compressive strength in pOC-ER α KO female L₅ vertebrae and with increased maximum moment in pOC-ER α KO male femora. Female pOC-ER α KO mice responded more to mechanical loading, whereas the response of pOC-ER α KO male animals was similar to their littermate controls. © 2015 American Society for Bone and Mineral Research. © 2015 American Society for Bone and Mineral Research.

KEY WORDS: GENETIC ANIMAL MODEL; SEX STEROIDS; OSTEOBLASTS; OSTEOPOROSIS

Introduction

Sex hormones are important regulators of bone mass in males and females. During puberty, estrogens inhibit, while androgens stimulate, periosteal bone formation in humans, contributing to generally higher bone mass in males.⁽¹⁾ The decline in estrogen associated with menopause is a primary contributor to postmenopausal osteoporosis in females.^(2–4) In men, sex hormone levels also decline with age and correlate with gradual bone loss.^(5–7) Estrogen signaling in bone occurs primarily through two estrogen receptors, estrogen receptor alpha (ER α) and estrogen receptor beta (ER β). Although both receptors are important in bone, a point mutation in ER α caused unfused growth plates and osteoporosis in a single reported human case.⁽⁸⁾ Since then, the role of ER α in

skeletal health in both males and females has become a major focus of research.^(9–11)

To better understand the role of estrogen in bone cells, global ER α knockout (ER α KO) and cell-specific ER α KO mice that remove ER α at specific points in the osteoblast-osteocyte lineage were developed, with conflicting outcomes concerning the cortical and cancellous bone status in males and females. With global deletion of ER α , cancellous and cortical tibial bone mineral density increased in females, but cortical and cancellous bone mass decreased in males.^(12–16) However, systemic effects that include altered hormone levels and body weight differences confound these results in global knockouts.^(14,16) When ER α was removed from osteoblast progenitors or precursors, using *Prx1*- or *Osx-Cre* mice, respectively,

Received in original form May 22, 2014; revised form February 17, 2015; accepted February 18, 2015. Accepted manuscript online Month 00, 2015.

Address correspondence to: Marjolein CH van der Meulen, PhD, Sibley School of Mechanical and Aerospace Engineering, Cornell University, 219 Upson Hall, Ithaca, NY 14853, USA. E-mail: mcv3@cornell.edu

Additional Supporting Information may be found in the online version of this article.

Journal of Bone and Mineral Research, Vol. xx, No. xx, Month 2015, pp 1–13

DOI: 10.1002/jbmr.2488

© 2015 American Society for Bone and Mineral Research

cortical bone mass decreased in females and young males, whereas cancellous bone was unaffected.⁽¹⁷⁾ ER α deletion in mature osteoblasts (OC-Cre) decreased cortical and cancellous bone mass,^(18,19) but bone mass was unchanged with deletion in committed osteoblasts in females (Col1a1-Cre).⁽¹⁷⁾ Bone mass in young and growing male mice was unaffected by ER α deficiency in osteoblasts in both targeted knockouts.^(18,19) Finally, when ER α was removed from osteocytes (Dmp1-Cre), female and male mice exhibited no change in or decreased bone mass, respectively.^(20,21)

Bone is mechanosensitive. Bone mass can increase in response to dynamic loading but decreases with disuse in adult animals.^(22,23) In vivo tibial and ulnar mechanical loading rodent models are established methods for studying the adaptive response of cancellous and cortical bone to controlled, dynamic bone loading.^(24–26) Although ER α has been implicated in bone mechanotransduction,^(27,28) the results were conflicting when the skeletal response to mechanical loading was examined in different bone cell–specific ER α KO mice. ER α in females had no effect on bone's anabolic response to mechanical loading when removed at the osteocyte stage of the lineage.⁽²⁰⁾ In Prx1-ER α KO and Osx-ER α KO mice, loading-induced periosteal expansion was reduced, whereas there was no difference in cortical adaptation to load in Col1-ER α KO mice.⁽²⁹⁾ In male animals, the response to mechanical loading has not been reported in any bone cell–specific ER α KO mouse. In all these models, the cancellous bone response to applied loading has not been reported.

No study to date has investigated cancellous and cortical bone adaptation to mechanical loading in male and female mice generated using the OC-Cre to remove ER α at the stage of mature osteoblasts and osteocytes (pOC-ER α KO). To generate these animals and littermate controls, we crossbred OC-Cre and ER α floxed mice. At 10 weeks of age, we subjected the left tibiae to 2 weeks of in vivo mechanical loading, with the right limb as an internal control, and analyzed bone mass and architecture through micro-CT, dynamic histomorphometry, and immunohistochemistry (IHC). In addition, we examined bone mass, morphology, and strength of L₅ vertebrae and femoral midshafts in LC and targeted animals. We hypothesized that ER α deficiency in mature osteoblasts and osteocytes would decrease bone mass in both female and male mice and that the response to mechanical loading would be attenuated in pOC-ER α KO mice. Our results did not fully support the hypothesis and revealed a more complex situation.

Materials and Methods

Generation of osteoblast-specific ER α KO mice

pOC-ER α KO and littermate control (LC) mice were bred and validated as previously described.⁽¹⁹⁾ Briefly, mice containing a transgene encoding Cre recombinase driven by the human osteocalcin promoter (OC-Cre, provided by Dr Thomas Clemens, The Johns Hopkins University, Baltimore, MD, USA)^(30,31) were crossed with mice in which exon 3 of the DNA-binding domain of the ER α gene (Esr1) was flanked by loxP sequences (ER α ^{fl/fl}, provided by Dr Kahn, University of Cincinnati, Cincinnati, OH, USA).⁽³²⁾ Before generation of pOC-ER α KO, ER α ^{fl/fl} mice were inbred to be >99% pure C57Bl/6 by speed congenics (DartMouse Speed Congenic Core Facility, Geisel School of Medicine at Dartmouth, Hanover, NH, USA). All mice were genotyped as described.⁽¹⁹⁾ Mice were housed 3 to 5 per cage

with *ad libitum* access to food and water. All animal procedures were approved by Cornell University's IACUC.

In vivo tibial mechanical loading

At 10 weeks of age, single-element strain gauges (EA-06-015LA-120, Micro-Measurements, Wendell, NC, USA) were surgically attached to the tibial midshafts of female and male LC and pOC-ER α KO mice ($n=5$ to 6 per genotype). A series of axial cyclic compressive loads (−2 to −12 N) were applied to the left and right tibiae in our custom tibial-loading device. Bone stiffness was calculated from the load and strain data as previously described⁽³³⁾ and used to calculate the peak load required to induce 1200 microstrain ($\mu\epsilon$) at the tibial midshaft during compressive axial tibial loading; strains at this location are well characterized. Bone stiffness was similar among pOC-ER α KO and LC male and female mice (0.00671 ± 0.0010 N/ $\mu\epsilon$ LC females, 0.00763 ± 0.00068 N/ $\mu\epsilon$ pOC-ER α KO females, 0.00760 ± 0.00029 N/ $\mu\epsilon$ LC males, 0.00767 ± 0.00016 N/ $\mu\epsilon$ pOC-ER α KO males). A peak load of −9.0 N was applied to all animals in the subsequent loading experiment.

The left tibiae of male and female LC and pOC-ER α KO mice ($n=12$ to 14 per group) were loaded in compression *in vivo* for 2 weeks.⁽³³⁾ In brief, a cyclic compressive load was applied at a rate of 4 Hz for 1200 cycles per day, 5 days per week, in a triangular waveform with a peak load of −9.0 N. A dwell of 100 ms at −0.5 N was maintained between successive load cycles, and the dwell-to-peak time was 75 ms, corresponding to a strain rate of 0.0016 ϵ /s at the tibial midshaft cortex. This methodology is well established in the literature.^(26,33,34)

Mass and serum marker measurements

Three days after the last day of mechanical loading, mice were euthanized via isoflurane overdose and cardiac puncture. Blood was stored overnight at 4°C and centrifuged at 1520 g for 20 minutes to separate serum. Serum was assayed ($n=8$ to 10 per group) for estrogen (E2, CalBiotech EW180S-100, Spring Valley, CA, USA), insulin-like growth factor 1 (IGF-1, ALPCO 22-IGF-R21, Salem, NH, USA), osteocalcin (OC, ALPCO 31-50-1300), tartrate-resistant acid phosphatase 5b (TRAP5b, IDS SB-TR103, Scottsdale, AZ, USA), and pro-collagen I N-terminal peptide (PINP, MyBioSource 703389, San Diego, CA, USA). Body mass and female uterine and ovarian masses were recorded at euthanasia.

Microcomputed tomography

Right femora and L₅ vertebrae were wrapped in PBS-soaked gauze and stored at −20°C before micro-CT scanning at 15 μm resolution ($\mu\text{CT}35$, Scanco Medical AG, Bruttisellen, Switzerland; 55 kVp, 145 μA , 600 ms integration time). Mineralized tissue was separated from nonmineralized tissue using sex- and bone-specific thresholds. The cancellous core and cortical shell of the vertebrae were analyzed as previously described.⁽¹⁹⁾ For the femur, a cortical volume of interest extending 0.5 mm, centered at the midshaft, was analyzed.

At euthanasia, left and right tibiae were stored overnight in 4% paraformaldehyde or 70% ethanol and then scanned in 70% ethanol at 15 μm voxel resolution ($\mu\text{CT}35$, Scanco Medical AG; 55 kVp, 145 μA , 600 ms integration time). For each tibia, the metaphyseal cancellous core and cortex were manually separated and analyzed. The metaphyseal region was defined from ~0.5 mm distal to the growth plate and extending distally

10% of total tibial length.⁽¹⁹⁾ The cortical midshaft was analyzed as previously described.⁽¹⁹⁾ The tibial midshaft was chosen to allow direct comparison to our previous work^(19,33) because this location corresponds to the site of in vivo tibial strain gauge calibration and because strains at the cortical midshaft are well established across vertebrates.⁽³⁵⁾

Cancellous bone outcome measures were bone volume fraction (BV/TV), trabecular thickness (Tb.Th), trabecular separation (Tb.Sp), and cancellous tissue mineral density (cn.TMD). Cortical bone outcome measures were cortical area (Ct.Ar), marrow area (Ma.Ar, tibial and femoral midshaft only), maximum and minimum moments of inertia (I_{MAX} , I_{MIN}), cortical thickness (Ct.Th), and cortical tissue mineral density (ct.TMD).

Dynamic histomorphometry

Ten and 3 days before euthanasia, mice ($n=6$ to 7 per group) received injections of calcein (30 mg/kg IP). After micro-CT scanning, tibiae were embedded in acrylosin and sectioned by the Bone Histology/Histomorphometry Laboratory (Yale University Department of Orthopaedics and Rehabilitation, New Haven, CT, USA). Both transverse sections of the tibial midshaft and longitudinal sections of the tibial metaphysis were analyzed to measure single and double fluorescent labels on bone surfaces (2 slides per animal, OsteomeasureXP v3.2.1.7, Osteometrics, Decatur, GA, USA). Measurable outcomes were mineralizing surface (MS), mineral apposition rate (MAR), bone formation rate (BFR), and woven bone area (Wo.Ar) at the periosteal and endosteal surfaces of the tibial midshaft and cancellous metaphysis according to ASBMR standards.⁽³⁶⁾ Woven bone regions were excluded from double-label analyses.

Table 1. Cancellous and Cortical Bone Were Differentially Affected in 10-Week-Old pOC-ER α KO Females and Males Measured by Micro-CT in the Vertebral Body, Vertebral Shell, and Femoral Midshaft

	Female		Male	
	LC	pOC-ER α KO	LC	pOC-ER α KO
Vertebral body				
BV/TV	0.189 \pm 0.029	0.160 \pm 0.015*	0.243 \pm 0.042	0.288 \pm 0.042
Tb.Th (μ m)	48.3 \pm 2.7	45.3 \pm 0.85*	50.2 \pm 5.1	53.9 \pm 5.0
Tb.Sp (μ m)	225 \pm 21	277 \pm 16	175 \pm 13	158 \pm 10*
Tb.N	4.40 \pm 0.37	4.40 \pm 0.27	5.49 \pm 0.28	5.96 \pm 0.29*
cn.TMD (mg HA/cc)	632 \pm 10	639 \pm 7.6	646 \pm 22	653 \pm 17
Vertebral shell				
Ct.Ar (mm^2)	0.329 \pm 0.0084	0.292 \pm 0.017*	0.321 \pm 0.043	0.329 \pm 0.029
Ct.Th (μ m)	65.5 \pm 3.0	58.0 \pm 2.0*	62.1 \pm 4.9	63.6 \pm 4.0
I_{MAX} (mm^4)	0.142 \pm 0.0088	0.139 \pm 0.014	0.136 \pm 0.019	0.141 \pm 0.020
I_{MIN} (mm^4)	0.0297 \pm 0.0026	0.0284 \pm 0.0025	0.0333 \pm 0.0073	0.0338 \pm 0.0044
ct.TMD (mg HA/cc)	791 \pm 7.5	787 \pm 8.1	795 \pm 6.3	798 \pm 9.0
Femoral midshaft				
Ct.Ar (mm^2)	0.726 \pm 0.027	0.675 \pm 0.021*	0.934 \pm 0.088	1.06 \pm 0.097*
Ma.Ar (mm^2)	0.890 \pm 0.046	0.908 \pm 0.053	1.17 \pm 0.096	1.24 \pm 0.13
Ct.Th (mm)	0.180 \pm 0.0040	0.167 \pm 0.0095*	0.193 \pm 0.0077	0.202 \pm 0.011
I_{MAX} (mm^4)	0.195 \pm 0.020	0.175 \pm 0.015*	0.351 \pm 0.063	0.430 \pm 0.072*
I_{MIN} (mm^4)	0.107 \pm 0.0077	0.103 \pm 0.0072	0.167 \pm 0.029	0.206 \pm 0.039*
ct.TMD (mg HA/cc)	945 \pm 8.9	933 \pm 9.1*	925 \pm 8.2	930 \pm 6.8

BV/TV = bone volume fraction; Tb.Th = trabecular thickness; Tb.Sp = trabecular separation; cn.TMD = cancellous tissue mineral density; Ct.Ar = cortical area; Ma.Ar = marrow area; Ct.Th = cortical thickness; I_{MAX} and I_{MIN} = maximum and minimum moments of inertia; ct.TMD = cortical tissue mineral density.

Data are mean \pm SD.

*pOC-ER α KO different from LC, $p < 0.05$ by one-factor ANOVA for each sex.

Histology

Left and right tibiae not used for dynamic histomorphometry were decalcified in 10% EDTA for 2 weeks, processed, and embedded in paraffin ($n=6$ to 7 per group). Tibias were sectioned longitudinally at 6 μ m using a rotary microtome (Leica RM2255, Wetzlar, Germany). Sections were stained for TRAP and pro-collagen I as previously described.⁽¹⁹⁾ The number of positively stained osteoclasts (TRAP) or osteoblasts (pro-collagen I) in the cancellous metaphysis was quantified and normalized to bone surface (2 slides/animal, OsteomeasureXP v3.2.1.7). Growth plate thickness was quantified from sections stained with Safranin O/Fast Green/Alcian Blue by averaging five evenly spaced lines (2 slides per mouse, $n=6$ mice/group, OsteomeasureXP v3.2.1.7).

Mechanical testing

Before mechanical testing, femora and L₅ vertebrae were thawed to room temperature and kept moist with PBS. Femora were tested in three-point bending to failure, and vertebrae were tested in compression to failure in the cranial-caudal direction as previously described (858 Mini Bionix, MTS, Eden Prairie, MN, USA).⁽¹⁹⁾ Whole-bone strength and stiffness were determined from the load-displacement data for bending and compression.

Statistics

For serum, bone lengths, in vivo bone stiffness, vertebral and femoral micro-CT, and mechanical testing data, a one-way ANOVA was used for each sex. To compare the loaded and control tibiae for tibial micro-CT, dynamic histomorphometry, histology, and IHC data, a repeated measures ANOVA with interaction was used on the absolute values for each sex with a

Table 2. Female 10-Week-Old pOC-ER α KO Mice Responded More to 2 Weeks of Tibial Compression Than LC, Whereas Male pOC-ER α KO Mice Responded Similarly to LC, Measured by Micro-CT in the Proximal Tibia and Tibial Midshaft

	Female		Male	
	LC	pOC-ER α KO	LC	pOC-ER α KO
Cancellous metaphysis				
BV/TV				
Control	0.0779 \pm 0.019 ^b	0.0584 \pm 0.0095 ^c	0.121 \pm 0.041 ^b	0.162 \pm 0.037 ^{*,a}
Loaded	0.111 \pm 0.014 ^{†,a}	0.115 \pm 0.015 ^{†,a}	0.143 \pm 0.030 ^{a,b}	0.156 \pm 0.016 ^{*,a,b}
Tb.Th (μ m)				
Control	48.4 \pm 2.4 ^c	46.4 \pm 2.2 ^{*,c}	46.0 \pm 5.2 ^c	52.4 \pm 5.6 ^{*,b}
Loaded	67.3 \pm 4.4 ^{†,b}	74.2 \pm 4.2 ^{*,†,a}	58.7 \pm 3.0 ^{†,a}	61.0 \pm 5.7 ^{*,†,a}
Tb.Sp (μ m)				
Control	323 \pm 35	413 \pm 41 [*]	227 \pm 28	225 \pm 36
Loaded	327 \pm 32	436 \pm 52 [*]	225 \pm 31	230 \pm 36
Tb.N				
Control	3.16 \pm 0.36	2.52 \pm 0.23 [*]	4.46 \pm 0.49	4.55 \pm 0.63
Loaded	3.09 \pm 0.26	2.39 \pm 0.25 [*]	4.41 \pm 0.61	4.41 \pm 0.59
cn.TMD (mg HA/cc)				
Control	767 \pm 13	757 \pm 14	765 \pm 9.1	774 \pm 15
Loaded	798 \pm 12 [†]	791 \pm 15 [†]	796 \pm 11 [†]	794 \pm 13 [†]
Cortical shell metaphysis				
Ct.Ar (mm^2)				
Control	0.964 \pm 0.092 ^b	0.866 \pm 0.050 ^b	1.11 \pm 0.12	1.18 \pm 0.14
Loaded	1.28 \pm 0.097 ^{†,a}	1.27 \pm 0.049 ^{†,a}	1.31 \pm 0.084 [†]	1.39 \pm 0.11 [†]
Ct.Th (mm)				
Control	0.141 \pm 0.010 ^b	0.128 \pm 0.0049 ^{*,c}	0.134 \pm 0.013	0.141 \pm 0.015
Loaded	0.179 \pm 0.011 ^{†,a}	0.174 \pm 0.0090 ^{*,†,a}	0.156 \pm 0.0076 [†]	0.158 \pm 0.0082 [†]
I _{MAX} (mm^4)				
Control	0.373 \pm 0.055	0.339 \pm 0.032	0.553 \pm 0.086	0.613 \pm 0.11 [*]
Loaded	0.534 \pm 0.070 [†]	0.540 \pm 0.047 [†]	0.670 \pm 0.063 [†]	0.771 \pm 0.12 ^{*,†}
I _{MIN} (mm^4)				
Control	0.301 \pm 0.040 ^b	0.268 \pm 0.035 ^c	0.421 \pm 0.061 ^b	0.440 \pm 0.061 ^b
Loaded	0.433 \pm 0.061 ^{†,a}	0.429 \pm 0.037 ^{†,a}	0.530 \pm 0.064 ^{†,a}	0.598 \pm 0.085 ^{†,a}
ct.TMD (mg HA/cc)				
Control	833 \pm 23	816 \pm 19	817 \pm 11	815 \pm 14
Loaded	843 \pm 20 [†]	883 \pm 12 [†]	827 \pm 17	815 \pm 7.8
Cortical midshaft				
Ct.Ar (mm^2)				
Control	0.560 \pm 0.029 ^c	0.534 \pm 0.026 ^c	0.769 \pm 0.080	0.823 \pm 0.053 [*]
Loaded	0.717 \pm 0.034 ^{†,b}	0.755 \pm 0.042 ^{†,a}	0.791 \pm 0.049 [†]	0.834 \pm 0.052 ^{*,†}
Ma.Ar (mm^2)				
Control	0.333 \pm 0.017	0.348 \pm 0.021	0.432 \pm 0.029 ^b	0.450 \pm 0.024 ^{*,ab}
Loaded	0.317 \pm 0.028 [†]	0.325 \pm 0.027 [†]	0.420 \pm 0.030 ^b	0.465 \pm 0.031 ^{*,a}
Ct.Th (mm)				
Control	0.205 \pm 0.0095 ^b	0.194 \pm 0.0062 ^b	0.241 \pm 0.018	0.249 \pm 0.012
Loaded	0.253 \pm 0.011 ^{†,a}	0.258 \pm 0.013 ^{†,a}	0.246 \pm 0.008	0.248 \pm 0.0072
I _{MAX} (mm^4)				
Control	0.0603 \pm 0.0054 ^c	0.0598 \pm 0.0065 ^{*,c}	0.121 \pm 0.022	0.141 \pm 0.017 [*]
Loaded	0.0926 \pm 0.0098 ^{†,b}	0.105 \pm 0.0089 ^{*,†,a}	0.127 \pm 0.017 [†]	0.1474 \pm 0.020 ^{*,†}
I _{MIN} (mm^4)				
Control	0.0505 \pm 0.0034 ^b	0.0470 \pm 0.0046 ^b	0.0849 \pm 0.014	0.0936 \pm 0.010 [*]
Loaded	0.0646 \pm 0.0064 ^{†,a}	0.0687 \pm 0.0057 ^{†,a}	0.0883 \pm 0.010 [†]	0.0985 \pm 0.012 ^{*,†}
ct.TMD (mg HA/cc)				
Control	1020 \pm 16	1020 \pm 8.4	1040 \pm 12	1050 \pm 17
Loaded	1010 \pm 18 [†]	1010 \pm 12 [†]	1040 \pm 11	1050 \pm 10

BV/TV = bone volume fraction; Tb.Th = trabecular thickness; Tb.Sp = trabecular separation; cn.TMD = cancellous tissue mineral density; Ct.Ar = cortical area; Ma.Ar = marrow area; Ct.Th = cortical thickness; I_{MAX} and I_{MIN} = maximum and minimum moments of inertia; ct.TMD = cortical tissue mineral density.

Data are mean \pm SD.

^{a,b,c}Groups not sharing the same letter are significantly different by Tukey HSD post hoc, where a $>$ b $>$ c. Post hoc performed when ANOVA interaction term was significant.

*pOC-ER α KO different from LC. [†]Loaded tibia different from Control, $p < 0.05$ by repeated measures ANOVA with interaction for each sex.

Tukey HSD post hoc test performed when the interaction term was significant. The between-subject factor was genotype, and the within-subject factor was loaded (left) versus control (right) limb. All statistical comparisons were made between sex-matched pOC-ER α KO and LC; females and males were not compared directly. Significance was set at $p < 0.05$. Increases and decreases among factors are reported as percentages in the text only when the absolute values from the statistical tests were significantly different.

Results

Physical characterization of pOC-ER α KO mice

We generated and examined male and female pOC-ER α KO and LC. Because the global ER α KO mouse possessed systemic effects that confound the role of ER α in bone alone,^(13,14,16,37) we measured body mass, crown/rump length, ovarian and uterine mass (females only), tibia and femur length, and serum levels of E2 and IGF-1 (Supplemental Fig. S1, Supplemental Table S1). All outcome measures were similar between pOC-ER α KO and LC within each sex, except for femoral length, which was greater in pOC-ER α KO males versus LC.

Female pOC-ER α KO mice exhibit decreased bone mass

To assess changes in bone structure and geometry, micro-CT analysis was performed on the L₅ vertebrae, femoral midshafts, and proximal and mid-diaphyseal control tibiae (Table 1, Table 2). Cancellous BV/TV was lower in pOC-ER α KO female mice by 16% in the vertebral

body and by 25% in the tibial metaphysis control limbs, attributable to lower Tb.Th in the vertebra (−6.2%) and increased Tb.Sp in the tibia (+28%) (Fig. 1, Table 2). Analogously, cortical bone at these two cortico-cancellous sites was also affected but to a lesser extent than the cancellous tissues. In the vertebral shell, both Ct.Ar (−11%) and Ct.Th (−11%) were lower in the knockouts compared with LC. From compression testing, the lower bone mass found in both cortical and cancellous regions of the pOC-ER α KO vertebra correlated with lower compressive strength (−18%), but compressive stiffness was unchanged. The tibial metaphyseal cortical shell was 9.3% thinner in female pOC-ER α KO mice.

At the tibial midshaft, the non-loaded right limbs in pOC-ER α KO female mice showed no difference from LC mice in Ct.Ar, Ct.Th, I_{MAX}, I_{MIN}, or other parameters (Table 2). At the femoral midshaft, however, Ct.Ar (−7.0%) and Ct.Th (−7.3%) were lower, as were I_{MAX} and ct.TMD (−10% and −1.3%, respectively) (Fig. 2, Table 1). These changes in bone geometry and architecture at the femoral midshaft did not result in changes in either maximum moment or bending stiffness in three-point bending tests in targeted mice compared with LC.

Male pOC-ER α KO mice exhibit increased bone mass

The bone phenotype found in male pOC-ER α KO mice compared with their littermate controls was opposite to that found in females (Tables 1 and 2). In the vertebral body, Tb.Sp was lower in knockouts (−9.9%), whereas Tb.Th remained unchanged, but these changes did not result in an overall alteration in BV/TV (Fig. 1). In the right tibial metaphysis, cancellous BV/TV was greater by 34%, owing largely to increased Tb.Th (+14%)

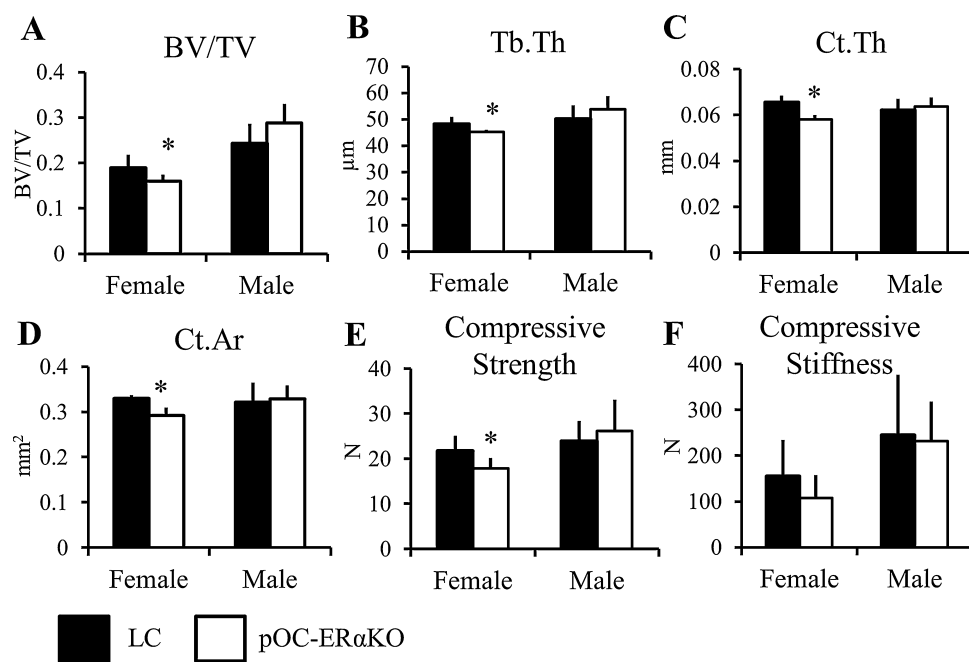


Fig. 1. Vertebral cancellous and cortical bone morphology and strength were differentially affected in 12-week-old pOC-ER α KO females and males compared with LC. (A) Vertebral body BV/TV was decreased because of decreased Tb.Th (B) in female knockouts compared with LC. (A) In male pOC-ER α KO mice, BV/TV in the vertebral shell was similar between genotypes. (C) The vertebral shell had thinner cortices in female pOC-ER α KO mice compared with LC, resulting in decreased Ct.Ar (D). Vertebral shell Ct.Ar and Ct.Th in pOC-ER α KO male mice were not different from LC. The cortical and cancellous morphology changes found in female and male pOC-ER α KO mice contributed to a decrease in compressive strength in vertebral compression tests in females but no change in compressive strength in male knockouts (E) or in compressive stiffness in either sex (F). BV/TV = bone volume fraction; Tb.Th = trabecular thickness; Ct.Ar = cortical area; Ct.Th = cortical thickness. Data are mean \pm SD, $n = 8$ to 12 per group. *pOC-ER α KO different from LC, $p < 0.05$ by one-way ANOVA for each sex.

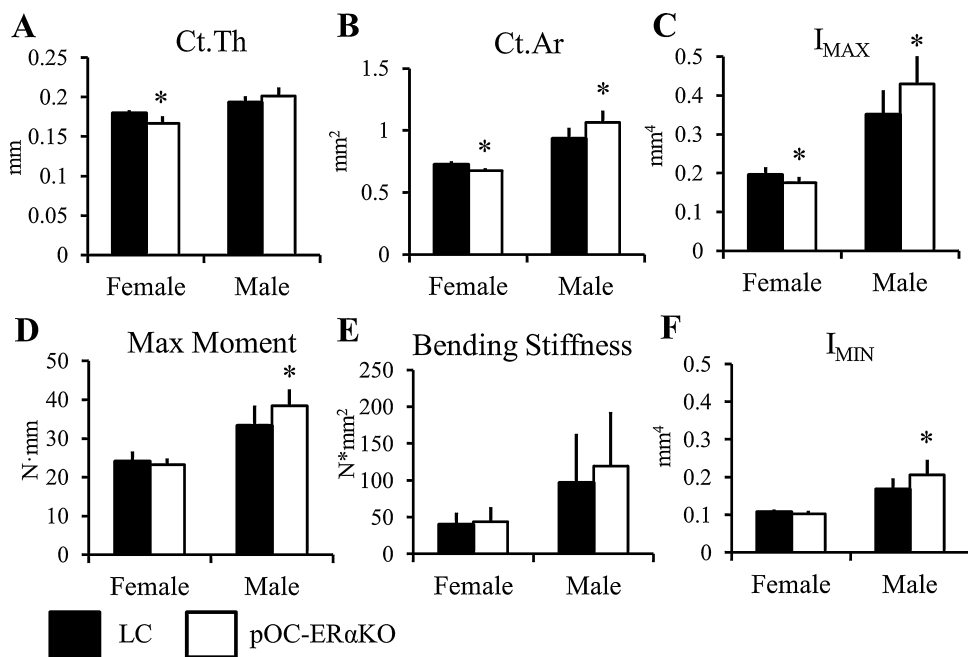


Fig. 2. Femoral midshaft bone morphology and strength were differentially affected in 12-week-old pOC-ER α KO females and males compared with LC. Female pOC-ER α KO mice had decreased Ct.Th (A), decreased Ct.Ar (B), and decreased I_{MAX} (C) compared with LC. (D, E) Maximum moment and bending stiffness were not different between genotypes in females from 3-point bending mechanical tests. Male pOC-ER α KO mice exhibited an opposite bone phenotype compared with LC than that found in females. Ct.Ar (B), I_{MAX} (C), and I_{MIN} (F) were all increased in male pOC-ER α KO mice, which resulted in increased maximum moment (D) in 3-point bending tests. Ct.Ar = cortical area; Ct.Th = cortical thickness; I_{MAX} and I_{MIN} = maximum and minimum moments of inertia. Data are mean \pm SD, $n = 8$ to 12 per group. *pOC-ER α KO different from LC, $p < 0.05$ by one-way ANOVA for each sex.

(Table 2). In the cortical shell of the tibial metaphysis, pOC-ER α KO mice had larger I_{MAX} (+15%) compared with LC but unchanged Ct.Ar, I_{MIN}, Ct.Th, and ct.TMD. The cortical shell of the vertebrae was unaffected by ER α deletion in osteoblasts and osteocytes. Compressive strength and stiffness were not different in pOC-ER α KO males compared with LC, reflecting the cortical bone mass and geometry at that site.

At two purely cortical regions, the right femoral and tibial midshafts, cortical bone mass was significantly greater in male pOC-ER α KO mice. In the femur, Ct.Ar (+14%), I_{MAX} (+23%), and I_{MIN} (+23%) were larger, which were reflected in greater maximum bending moment (+15%) but with no change in whole-bone stiffness from bending tests (Fig. 2). Similarly, at the right tibial midshaft, male pOC-ER α KO mice had larger Ct.Ar (+6.9%), I_{MAX} (+16%), and I_{MIN} (+10%).

ER α in osteoblasts and osteocytes suppresses the anabolic response to mechanical loading in female mice

At the tibial metaphysis, cancellous bone responded robustly to mechanical loading in both LC and gene-deleted females (Fig. 3). BV/TV, Tb.Th, and cn.TMD were increased after 2 weeks of loading (Table 2). Matrix-secreting osteoblast activity from pro-collagen-I IHC normalized to bone surface was increased in loaded versus control tibiae (Figs. 4 and 5), as expected from new bone formation resulting from loading. Osteoclast number measured by TRAP histology normalized to bone surface was not affected by loading or by genotype (Fig. 4). Tibial growth plate thickness increased with loading and was increased in control limbs of knockouts compared with control limbs of LC (Table 3).

Both BV/TV and Tb.Th increased significantly more in response to mechanical loading in mice lacking ER α in mature osteoblasts and osteocytes than in LC. BV/TV increased 97% in pOC-ER α KO and only 43% in LC, owing to increased Tb.Th (+60%, +39%, respectively). Although BV/TV was lower in knockout mice in the control limbs compared with LC, Tb.Th was not different between control right tibiae. Dynamic histomorphometry results showed that MAR in the cancellous metaphysis increased more in pOC-ER α KO females in response to 2 weeks of loading than in LC mice, analogous to the increased loading response found in the micro-CT data (Table 3, Fig. 4, Supplemental Fig. S2). MS and BFR increased similarly with loading in both genotypes.

Similar to the cancellous region of the tibial metaphysis, Ct.Ar, Ct.Th, I_{MAX}, I_{MIN}, and ct.TMD in the cortical shell of the tibial metaphysis increased in response to mechanical loading. Both I_{MIN} and Ct.Th were decreased in the control tibiae of pOC-ER α KO female mice compared with LC, and these two parameters responded significantly more to mechanical loading in pOC-ER α KO mice. I_{MIN} increased 64% in pOC-ER α KO but only 44% in LC. Ct.Th increased 37% in knockouts but only 27% in LC. Ct.Ar responded similarly to mechanical loading as LC and was not different in right control limbs.

At the tibial midshaft, female pOC-ER α KO mice responded more to mechanical loading than LC despite having similar bone architecture in contralateral limbs (Fig. 6). Ct.Ar increased more in pOC-ER α KO mice (+41%) than in LC (+28%), as did I_{MAX} (+76% in pOC-ER α KO and +53% in LC) (Table 2). Ct.Th, I_{MIN}, and ct.TMD increased similarly between genotypes with 2 weeks of tibial loading. New bone formed on both the periosteal and endosteal surfaces of the tibial midshaft, as indicated by

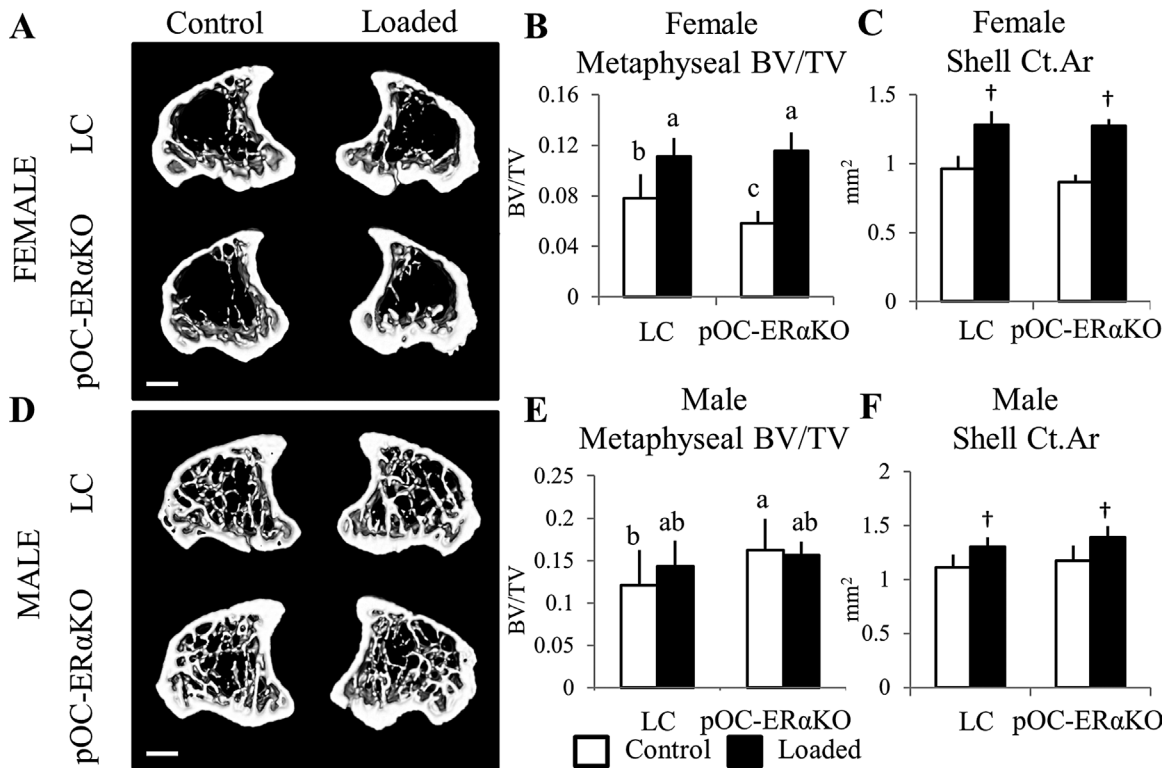


Fig. 3. Tibial metaphyseal bone mass was reduced in pOC-ER α KO female mice but increased in pOC-ER α KO male mice, and pOC-ER α KO female mice responded more to 2 weeks of tibial compression. Representative transverse 3D micro-CT reconstructions (0.51 mm thick) of the tibial metaphysis in female (A) and male (D) 12-week-old LC (top) and pOC-ER α KO mice (bottom) after 2 weeks of left tibial loading. (B) BV/TV of cancellous bone in female pOC-ER α KO mice was 25% lower in the unloaded right tibia compared with LC. After 2 weeks of tibial loading, BV/TV increased more (+97%) in pOC-ER α KO mice than in LC mice (+43%). (E) BV/TV was increased in the tibial metaphysis of male pOC-ER α KO compared with LC, but 2 weeks of loading did not alter BV/TV in left versus right limbs for either genotype. (C, F) Area of the cortical shell increased similarly between genotypes within each sex after loading, and Ct.Ar was unaffected by ER α deletion in both sexes. BV/TV = bone volume fraction; Ct.Ar = cortical area. Data are mean \pm SD, $n = 12$ to 14 per group. † Loaded tibia different from Control, $p < 0.05$ by repeated measures ANOVA with interaction for each sex. Bars not sharing same letter are significantly different from one another from Tukey HSD post hoc only when interaction term (load*genotype) was significant. Scale bar = 1.0 mm.

increased MS, MAR, and BFR at the periosteum and increased MAR and BFR at the endosteum (Table 3, Supplemental Fig. S2). As such, Ma.Ar decreased with loading (-4.9% pOC-ER α KO, -6.5% LC). Of note, woven bone formation was present at the tibial midshaft of both genotypes of female mice in response to loading but not in the metaphysis. Micro-CT measurements at the tibial midshaft included both woven and lamellar bone, whereas the histomorphometric data (MS, MAR, and BFR) excluded woven bone.

Global measures of bone formation and osteoblast activity, such as serum P1NP and OC levels, were not different between genotypes (Supplemental Fig. S1), consistent with local measures of matrix production by osteoblasts in the cancellous metaphysis (matrix secreting N.Ob/BS) and dynamic histomorphometry measurements at both the cancellous metaphysis and tibial midshaft. The latter data differed only in MAR, which was decreased in the cancellous metaphysis of control tibiae of knockout animals.

Response to mechanical loading is unchanged in male pOC-ER α KO mice

After 2 weeks of tibial loading in male mice, cancellous trabeculae thickened ($+16\%$ pOC-ER α KO, $+28\%$ LC) and cn.

TMD increased ($+2.6\%$ pOC-ER α KO, $+4.0\%$ LC) in the loaded limb compared with the contralateral limb in both genotypes in the tibial metaphysis (Table 2). Overall BV/TV did not increase with loading as in previous similar experiments with male C57Bl/6 mice, although Tb.Th did increase^(26,38) (Fig. 3). Activity of matrix-secreting osteoblasts and osteoclast number normalized to bone surface, indicative of increased turnover, were both increased in loaded versus contralateral tibial metaphyses, as was tibial growth plate thickness (Table 3, Fig. 4). Cancellous MS increased in pOC-ER α KO and LC with loading, but MAR and BFR were unchanged (Table 3, Fig. 4, Supplemental Fig. S2).

In the cortical shell of the metaphysis, Ct.Ar, I_{MAX} , and I_{MIN} increased in response to 2 weeks of mechanical loading compared with control limbs. Despite pOC-ER α KO mice having higher bone mass in the cancellous metaphysis and increased I_{MAX} in the cortical shell metaphysis, LC and pOC-ER α KO showed similar responses to in vivo tibial loading.

At the cortical tibial midshaft, Ct.Ar increased 1.4% in pOC-ER α KO with loading and 2.8% in LC (Fig. 6). Most new bone formation reflected periosteal expansion, as shown through increased periosteal MS and MAR, but no change in marrow area (Table 3). However, endosteal MS increased with loading in both genotypes, whereas I_{MAX} and I_{MIN} also were higher. Cortical

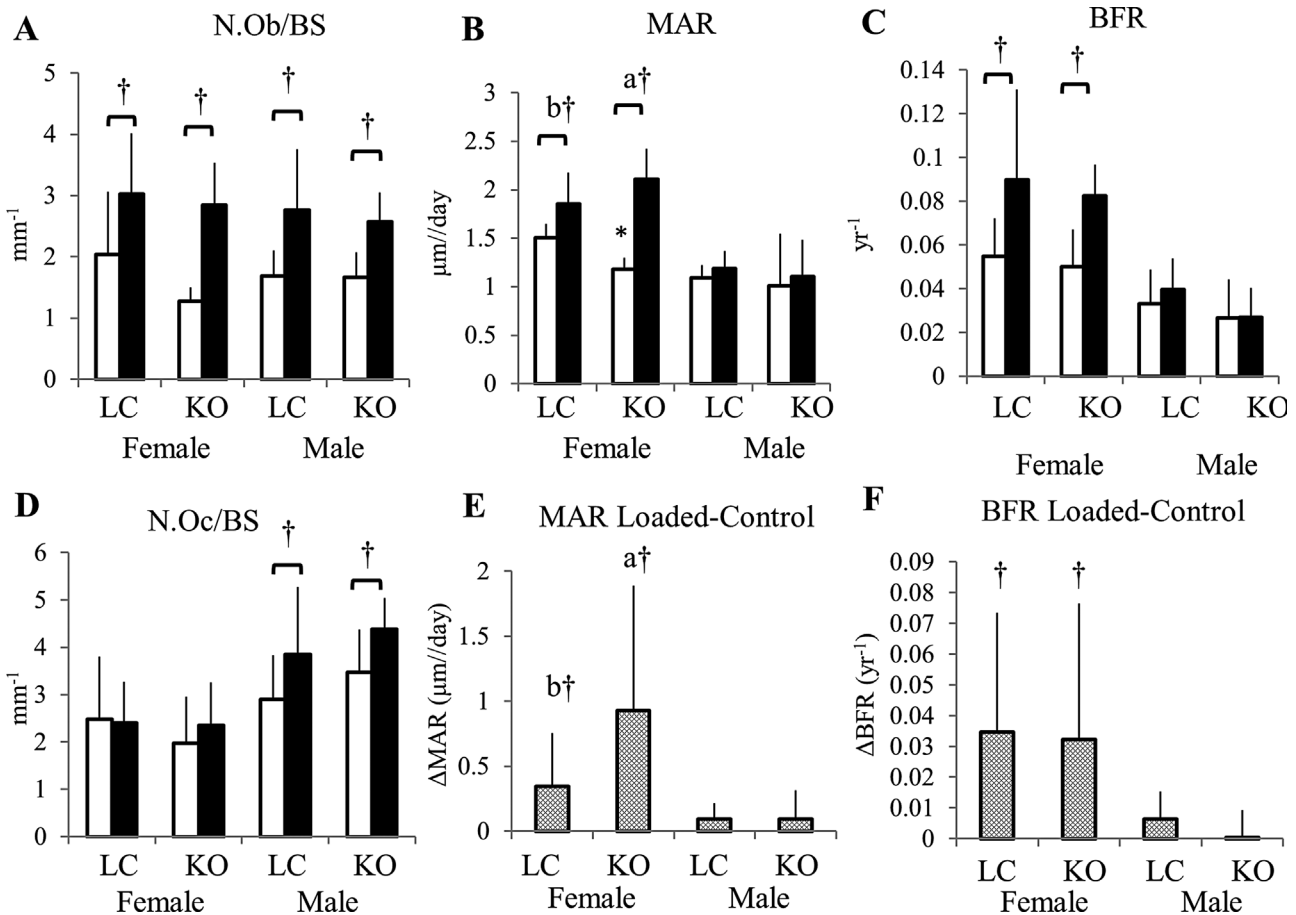


Fig. 4. (A) Two weeks of loading increased matrix-secreting N.Ob/BS in the cancellous tibial metaphysis in both genotypes and sexes. In female mice, MAR (B, E) and BFR (C, F) were increased with loading, and MAR increased more in pOC-ER α KO than in LC mice (B, E). In male mice, MAR and BFR were not affected by tibial loading. (D) N.Oc/BS increased after loading in male but not female mice. Matrix-secreting N.Ob/BS = number of osteoblasts staining positively for pro-collagen I normalized to bone surface; N.Oc/BS = number of osteoclasts staining positively for TRAP normalized to bone surface; MAR = mineral apposition rate; BFR = bone formation rate. Data are mean \pm SD, $n = 6$ to 7 per group. *pOC-ER α KO different from LC. †Loaded tibia different from Control, $p < 0.05$ by repeated measures ANOVA with interaction for each sex. Bars not sharing same letter are significantly different from one another from Tukey HSD post hoc only when interaction term (load*genotype) was significant.

geometry in pOC-ER α KO male mice responded similarly to mechanical loading as LC mice.

Serum levels of PINP and TRAP5b were similar between genotypes, analogous to local activity of matrix-secreting osteoblasts and osteoclast number, but serum levels of OC were decreased in male pOC-ER α KO mice in the face of higher bone mass (Supplemental Fig. S1).

Discussion

We generated 10-week-old female and male mice lacking ER α in mature osteoblasts and osteocytes by breeding $ER\alpha^{fl/fl}$ and OC-Cre mice. Serum measurements, bone lengths, and growth plate analyses revealed that systemic effects were not present in females and limited in males, who showed increased femur length. When ER α was removed in mature osteoblasts and osteocytes, cancellous and cortical bone mass were lower at most sites in females; in contrast, pOC-ER α KO male mice had increased cancellous and cortical bone mass. When mice were subjected to 2 weeks of in vivo mechanical tibial loading, female

pOC-ER α KO mice formed more bone in response to loading than LC. In contrast, genotype did not affect the skeletal response to mechanical loading in males.

Although osteoblast-specific ER α KO mice do not have the confounding systemic effects of global ER α KO mice, the possibility of other compensating mechanisms cannot be ruled out. When both ER α and ER β are present, their functions are hypothesized to have minimal overlap. However, in global ER α KO mice, ER β may mediate gene transcription normally controlled by ER α .⁽³⁹⁾ ER β has also been implicated in the skeletal response to mechanical loading and could compensate for lack of ER α .^(12,40)

ER α in osteoblasts and osteocytes clearly has a role in bone mass accrual and its response to mechanical loading. Our previous work and that of Määttä and colleagues found similarly reduced bone mass in female mice when ER α was deleted in mature osteoblasts and osteocytes using the OC-Cre-driven promoter.^(18,19) Määttä and colleagues did not find genotype differences in males, except at 6 months of age, at which time tibial BV/TV and Tb.N were lower in knockouts. Genetic background can profoundly affect bone structure and

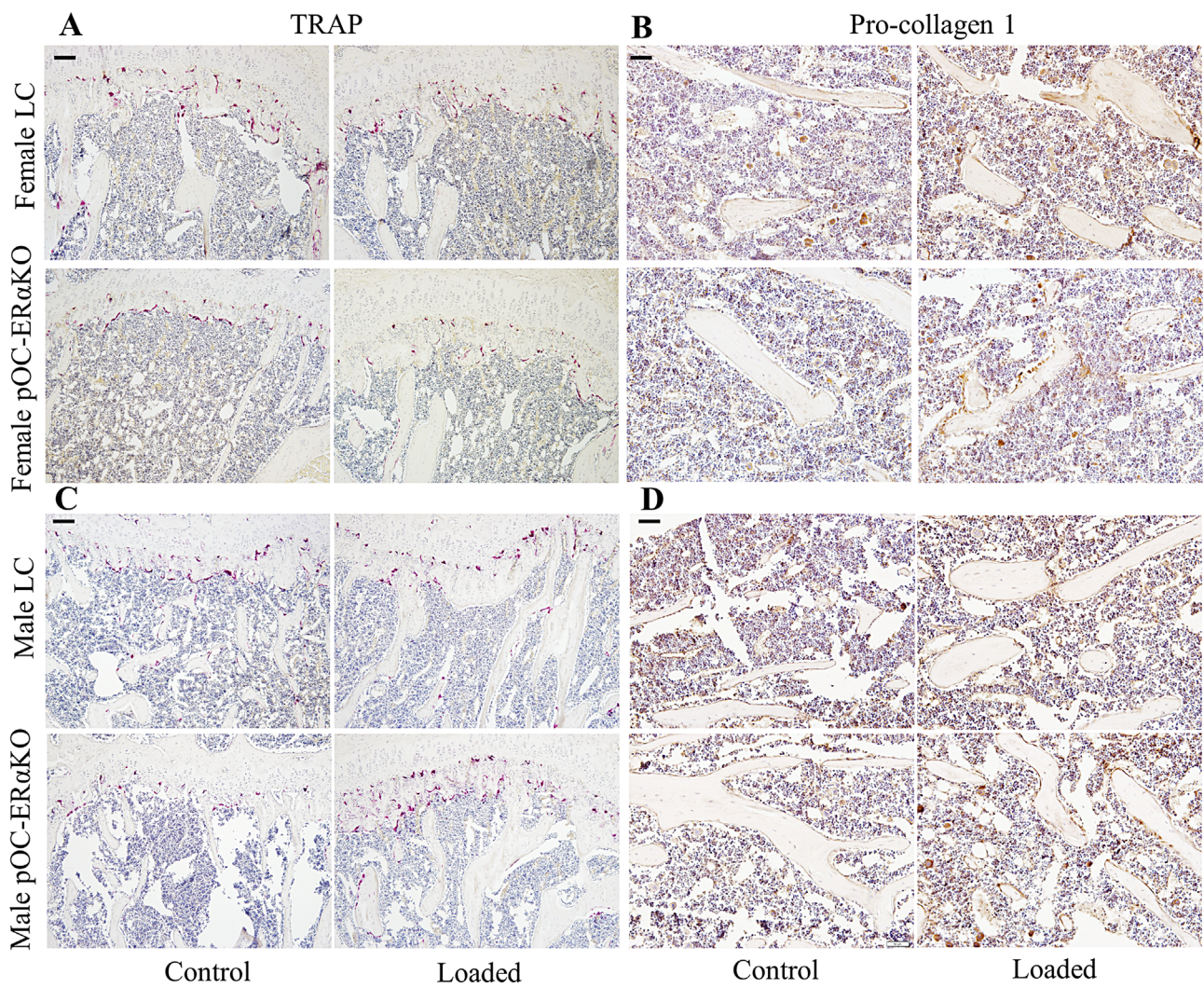


Fig. 5. Representative IHC and histology images for sagittal sections of the proximal tibiae of female (top) and male (bottom) LC and pOC-ER α KO mice in loaded and control limbs. (A) N.Oc/BS was not altered by genotype or loading in female mice. (B) N.Ob/BS increased with 2 weeks of in vivo tibial loading similarly in both genotypes. (C, D) Osteoclast number and osteoblast activity normalized to bone surface both increased after 2 weeks of in vivo tibial mechanical loading in male pOC-ER α KO and LC mice. Matrix-secreting N.Ob/BS = number of osteoblasts staining positively for pro-collagen I normalized to bone surface; N.Oc/BS = number of osteoclasts staining positively for TRAP normalized to bone surface. Scale bars = 80 μ m (A, C); 20 μ m (B, D).

mass.^(41,42) Our mice were backcrossed fully to a C57Bl/6 background, whereas the background of those studied by Määttä and colleagues was not reported. Of note, our current study examined 10-week-old mice, whereas the Määttä study analyzed older mice at 3.5, 6, and 12 months of age. We have shown previously that age at the time of loading influences bone adaptation and does so differently in the cortical mid-diaphysis and cancellous metaphysis.⁽⁴³⁾ We chose to examine 10-week-old mice that are still growing and whose proximal tibia contains a substantial volume of cancellous bone that is responsive to loading. Including skeletally mature and aged mice in future studies will provide a more complete picture of the role of ER α in osteoblasts and osteocytes.

During puberty, sex steroids promote bone growth and are major contributors to sexual skeletal dimorphism in humans.⁽¹⁾ Late in puberty, estrogen suppresses periosteal apposition and leads to growth plate fusion in both sexes.^(44,45) Adult males

have greater bone mass because of a prolonged puberty and high testosterone levels that increase periosteal apposition.⁽⁴⁶⁾ In pOC-ER α KO male mice, because the growth-suppressive effects of estrogen do not act on mature osteoblasts or osteocytes via ER α , the stimulating effects of testosterone on bone growth may be enhanced and might help to explain the higher bone mass phenotype found in these animals. Females lacking an estrogenic response via ER α in mature osteoblasts and osteocytes may accrue bone mass during growth more slowly, resulting in the decreased bone mass found in female pOC-ER α KO mice.

Our findings indicate that ER α mediates mechanosensitivity in bone of female mice. We found that both cortical and cancellous adaptation to load were greater in pOC-ER α KO female mice but unchanged in pOC-ER α KO male mice compared with sex-matched controls. At the cancellous metaphysis, the effect of the reduced bone mass on the tissue strains is unclear. With similar

Table 3. Two Weeks of Daily Tibial Loading Increased Cancellous, Periosteal, and Endosteal MAR and BFR of 10-Week-Old Female pOC-ER α KO and LC mice (Dynamic Histomorphometry, Histology, and Immunohistochemistry Data for Tibia in Female and Male pOC-ER α KO and LC Mice)

	Female		Male	
	LC	pOC-ER α KO	LC	pOC-ER α KO
Cn.MS				
Control	0.210 \pm 0.033 ^{bc}	0.231 \pm 0.040 ^c	0.276 \pm 0.046	0.250 \pm 0.059
Loaded	0.325 \pm 0.041 ^{†,ab}	0.279 \pm 0.034 ^{†,a}	0.320 \pm 0.025 [†]	0.279 \pm 0.086 [†]
Cn.MAR (μm/d)				
Control	1.51 \pm 0.14 ^b	1.18 \pm 0.12 ^b	1.09 \pm 0.13	1.01 \pm 0.53
Loaded	1.85 \pm 0.33 ^{†,ab}	2.11 \pm 0.31 ^{†,a}	1.19 \pm 0.18	1.10 \pm 0.38
Cn.BFR (yr$^{-1}$)				
Control	0.0550 \pm 0.017	0.0502 \pm 0.017	0.0331 \pm 0.016	0.0266 \pm 0.018
Loaded	0.0897 \pm 0.041 [†]	0.0396 \pm 0.014 [†]	0.0825 \pm 0.014	0.0270 \pm 0.013
Es.MS				
Control	0.587 \pm 0.029	0.551 \pm 0.186	0.357 \pm 0.19	0.195 \pm 0.12 [*]
Loaded	0.556 \pm 0.16	0.380 \pm 0.10	0.312 \pm 0.19 [†]	0.137 \pm 0.059 ^{*†}
Es.MAR (μm/d)				
Control	0.825 \pm 0.19	0.710 \pm 0.37	0.438 \pm 0.37	0.320 \pm 0.37
Loaded	2.08 \pm 0.57 [†]	1.47 \pm 0.43 [†]	0.529 \pm 0.72	0.143 \pm 0.35
Es.BFR (yr$^{-1}$)				
Control	0.0669 \pm 0.014 ^b	0.0605 \pm 0.038 ^{*b}	0.0241 \pm 0.017	0.0106 \pm 0.015
Loaded	0.198 \pm 0.076 ^{†,a}	0.105 \pm 0.037 ^{*†,a}	0.0323 \pm 0.045	0.00282 \pm 0.007
Es.Wo.Ar (mm2)				
Control	0.00 \pm 0.0	0.00 \pm 0.0	0.00 \pm 0.0	0.00 \pm 0.0
Loaded	0.0105 \pm 0.015 [†]	0.0223 \pm 0.014 [†]	0.00 \pm 0.0	0.00 \pm 0.0
Ps.MS				
Control	0.105 \pm 0.060	0.0827 \pm 0.032	0.0839 \pm 0.045	0.211 \pm 0.17
Loaded	0.226 \pm 0.081 [†]	0.260 \pm 0.11 [†]	0.431 \pm 0.23 [†]	0.413 \pm 0.15 [†]
Ps.MAR (μm/d)				
Control	0.00 \pm 0.0	0.00 \pm 0.0	0.00 \pm 0.0	0.147 \pm 0.36
Loaded	2.34 \pm 0.19 [†]	1.70 \pm 0.91 [†]	1.02 \pm 0.95 [†]	0.775 \pm 0.48 [†]
Ps.BFR (yr$^{-1}$)				
Control	0.00 \pm 0.0	0.00 \pm 0.0	0.00 \pm 0.0	0.00596 \pm 0.015
Loaded	0.0964 \pm 0.019 [†]	0.0774 \pm 0.040 [†]	0.0552 \pm 0.053	0.0270 \pm 0.019
Ps.Wo.Ar (mm2)				
Control	0.00 \pm 0.0	0.00 \pm 0.0	0.00 \pm 0.0	0.00 \pm 0.0
Loaded	0.140 \pm 0.028 [†]	0.166 \pm 0.049 [†]	0.00525 \pm 0.012	0.00 \pm 0.0
N.Ob/BS (mm$^{-1}$)				
Control	2.48 \pm 1.0	1.27 \pm 0.23	1.68 \pm 0.42	1.67 \pm 0.41
Loaded	3.02 \pm 1.0 [†]	2.84 \pm 0.69 [†]	2.77 \pm 0.99 [†]	2.57 \pm 0.48 [†]
N.Oc/BS (mm$^{-1}$)				
Control	2.48 \pm 1.3	1.97 \pm 0.98	2.90 \pm 0.93	3.47 \pm 0.91
Loaded	2.41 \pm 0.87	2.35 \pm 0.91	3.85 \pm 1.4 [†]	4.38 \pm 0.66 [†]
GP.Th (μm)				
Control	107 \pm 8.5	119 \pm 2.7 [*]	106 \pm 15	119 \pm 10
Loaded	178 \pm 5.0 [†]	198 \pm 17 ^{*†}	187 \pm 15 [†]	180 \pm 34 [†]

Cn = cancellous; Es = endosteal; Ps = periosteal; MS = mineralizing surface; MAR = mineral apposition rate; BFR = bone formation rate; N.Ob/BS and N.Oc/BS = number of matrix-secreting osteoblasts positively stained for pro-collagen 1 or positively stained osteoclasts with TRAP normalized to bone surface; GP.Th = growth plate thickness.

Data are mean \pm SD.

^{a,b,c}Groups not sharing the same letter are significantly different by Tukey HSD post hoc, where a $>$ b $>$ c. Post hoc performed when ANOVA interaction term was significant.

*pOC-ER α KO different from LC. [†]Loaded tibia different from Control, $p < 0.05$ by repeated measures ANOVA with interaction for each sex.

loading on less bone mass, the strains could be increased, producing an increased adaptive response; alternately, the reduced bone mass could reduce load sharing and reduce the strain in the tissue. Our results are in contrast to other studies examining the role of ER α in mechanotransduction. For example, in osteoblast cultures, cells lacking ER α responded

less to mechanical strain.⁽⁴⁷⁾ Similarly, the cortical response to mechanical loading was decreased in global ER α KO female mice and in female mice with ER α deleted at the osteoblast progenitor and osteoblast precursor stages compared with controls.^(12,29,48) In mice with ER α deleted at the committed osteoblast stage or the osteocyte stage, the cortical response to

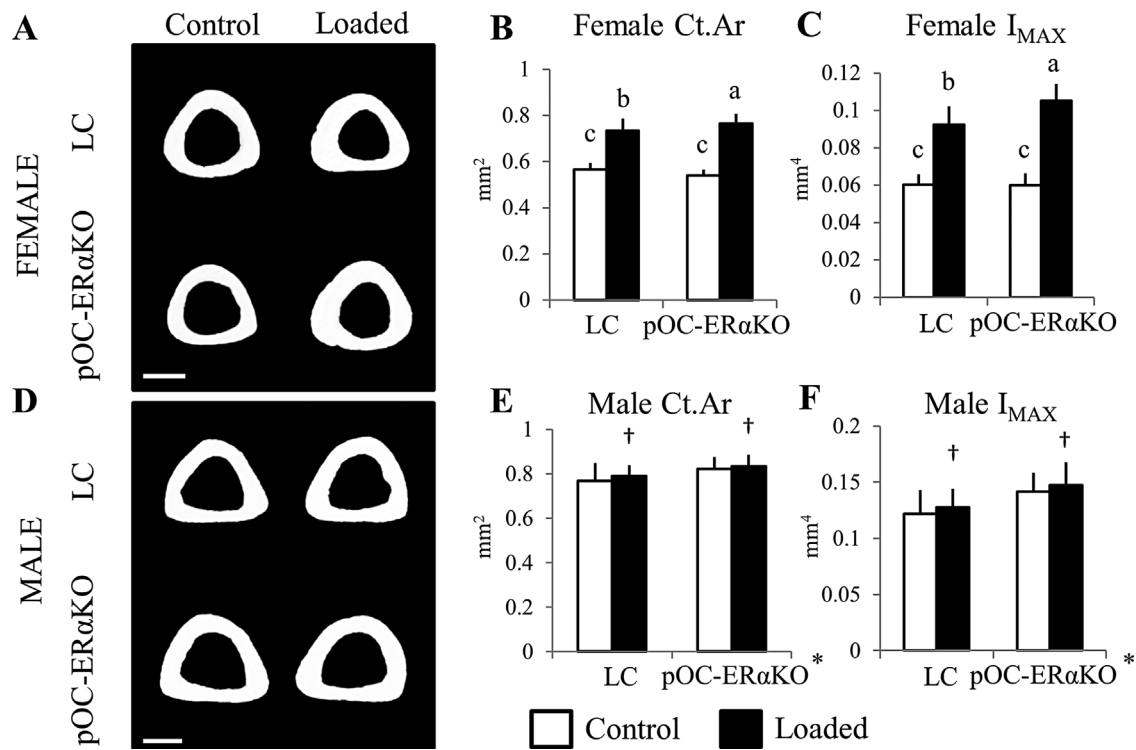


Fig. 6. Tibial midshaft cortical bone mass was similar between pOC-ER α KO and LC mice, but knockouts responded more to 2 weeks of tibial loading. Representative transverse 3D micro-CT reconstructions (45 μ m thick) of the tibial midshaft in female (A) and male (D) 12-week-old LC (top) and pOC-ER α KO mice (bottom) after 2 weeks of left tibial loading. (B, C) Although Ct.Ar was not different between LC and pOC-ER α KO female mice in the right, control limb, after 2 weeks of tibial loading, Ct.Ar increased more in pOC-ER α KO mice (+41%) versus LC (+28%), as did I_{MAX}. (E, F) Male pOC-ER α KO mice had increased Ct.Ar and I_{MAX} at the tibial midshaft in the right unloaded limbs, and both genotypes showed a similar increase in Ct.Ar and I_{MAX} after 2 weeks of mechanical loading. Ct.Ar = cortical area; I_{MAX} = maximum moment of inertia. Data are mean \pm SD, $n = 12$ to 14 per group. *pOC-ER α KO different from LC. †Loaded tibia different from Control, $p < 0.05$ by repeated measures ANOVA with interaction for each sex. Bars not sharing same letter are significantly different from one another from Tukey HSD post hoc only when interaction term (load*genotype) was significant. Scale bar = 0.5 mm.

mechanical loading was unchanged in female mice.^(20,29) However, other researchers have indicated that estrogen and/or ER α may inhibit the skeletal response to mechanical loading, in agreement with our work. Kondoh and colleagues performed hindlimb unloading in Dmp1-ER α KO female mice and showed an accelerated loss of bone mass compared with littermate controls.⁽²¹⁾ Furthermore, whole-body vibration increased periosteal and endosteal perimeters in ovariectomized rat tibiae but not in sham control tibiae.⁽⁴⁹⁾ Based on these prior results and our data, we conclude that the absence of ER α in mature osteoblasts and/or osteocytes of female mice did not reduce but maintained or enhanced sensitivity to the loading environment in ER α -deficient bone.⁽⁴⁵⁾

The formation of woven bone in response to mechanical loading at both the periosteal and endosteal surfaces of the tibial midshaft in female pOC-ER α KO and LC mice is a limitation of this study, as we aimed to analyze lamellar bone formation from skeletal loading. A peak load of \sim 9.0 N was required to produce 1200 μ e at the midshaft cortex, and similar load levels have been used previously for mouse tibial loading.^(33,34) After mechanical loading, the amount and variety of differentially expressed genes depends on whether lamellar or woven bone is being generated.⁽⁵⁰⁾ The possible effects of woven versus lamellar bone on data interpretation at the cortex from the

current study cannot be discounted. Findings at the tibial midshaft of this study cannot be directly compared with other studies investigating lamellar bone formation at the tibial midshaft. The similar increases in MS, MAR, and BFR at the periosteum between genotypes were unexpected given that the micro-CT data showed that Ct.Ar and I_{MAX} increased more in response to loading in pOC-ER α KO versus LC female mice. However, the presence of woven bone prevented quantification of single- and double-labeling along \sim 25% of the periosteal surface, thus the differences in loading response in pOC-ER α KO females may have been obscured. Both woven and lamellar bone were included in micro-CT measures, whereas woven bone regions were excluded from the histomorphometric analyses.

Female pOC-ER α KO also responded more to mechanical loading in the proximal tibia, where woven bone was not present and where Ct.Ar was similar between genotypes, indicating that ER α does regulate the skeletal response to mechanical loading during accrual of lamellar bone. Bone mass in the cancellous proximal tibia of pOC-ER α KO female mice was lower than that of LC mice. Because load levels were normalized for a target strain level at the cortical midshaft, a site at which bone mass and stiffness were similar between genotypes, we cannot distinguish whether the increased response to mechanical load in the cancellous tissues of the female pOC-ER α KO was

caused purely by genotypic effects or a combination of genotype and different strains in the cancellous tissues of the knockouts relative to the LC.

Male pOC-ER α KO mice responded similarly to loading as LC mice in the cancellous metaphysis, the cortical shell of the proximal tibia, and the tibial midshaft. Although Tb.Th increased with loading in both genotypes in the cancellous metaphysis, surprisingly overall BV/TV was unchanged. One possible explanation for the dampened loading response in the cancellous metaphysis could be the group housing of our male mice. Recently, group-housed males had an attenuated response to mechanical loading compared with single-housed males that was attributed to cage fighting.⁽⁵¹⁾ However, those mice were recently purchased and housed together, whereas the mice in the current study were group-housed for months after breeding in-house and thus less likely to fight. Also, this same loading protocol increased cancellous bone mass in recently purchased 10-week-old C57Bl/6 male mice previously.⁽³³⁾ Furthermore, the current loading study did produce an anabolic response to loading in male mice at both cortical sites analyzed. The lack of change of BV/TV in the proximal tibia with loading in the male animals is unexpected and requires further investigation.

Use of a cre-recombinase driven by the OC promoter (pOC) has been widely used in the literature.⁽³¹⁾ Although the OC-Cre mouse has been a tool to knock out specific receptors and proteins in mature osteoblasts and subsequent osteocytes, cre expression has been detected in the growth plate.⁽⁵²⁾ Previously in our mixed-background strain of female pOC-ER α KO mice, we found no differences in growth plate thickness or in tibial or femoral lengths compared with LC.⁽¹⁹⁾ However, in the current animals, on a pure C57Bl/6 background, female pOC-ER α KO mice had thicker tibial growth plates but no differences in tibial or femoral bone length. In contrast, although growth plate thickness was the same in pOC-ER α KO males, femoral length was increased but tibial length was unaffected. Määttä and colleagues found increased tibial lengths in male pOC-ER α KO mice at 3 months of age.⁽¹⁸⁾ These results are difficult to interpret because mouse growth plates never fuse. Thus, OC-Cre expression in the growth plate may affect growth plate thickness and bone length. However, overall body mass and crown/rump length were not altered in pOC-ER α KO mice of either sex.

Because declining sex hormones contribute greatly to osteoporosis in the elderly, especially postmenopausal women who have severely decreased estrogen levels, recent research has focused on understanding the role of estrogen signaling via its receptors in bone.⁽⁹⁾ Here ER α in mature osteoblasts and osteocytes differentially regulated bone mass in males and females. Removing ER α increased the skeletal response to mechanical loading at cortical and cancellous sites in females but did not affect skeletal adaption to physical stimuli in male mice. Further research should emphasize elucidating the cellular mechanisms and signaling pathways involved in estrogen signaling in bone, which may provide valuable insight into the pathogenesis of osteoporosis.

Disclosures

All authors state that they have no conflicts of interest.

Acknowledgments

We acknowledge Funmi Adebayo, Frank Ko, and Cornell CARE Staff for their assistance. We thank Dr Thomas Clemens for

providing OC-Cre mice and Dr Sohaib Khan for providing ER α ^{f/f} mice.

Financial support was provided by National Institutes of Health grants R01-AG028664 and P30-AR046121 (MCHM), NSF GRFP (KMM and NHK), and F32-AR054676 (RPM).

Authors' roles: Study design: KMM, FPR, and MCHM. Study conduct: KMM, NHK, and DBB. Data collection: KMM, NHK, GS, and DBB. Data analysis: KMM. Data interpretation: KMM, MCHM, and FPR. Drafting manuscript: KMM. Revising manuscript content: KMM, MCHM, FPR, and RPM. Approving final version of manuscript: all authors. KMM takes responsibility for the integrity of the data analysis.

References

1. Callewaert F, Sinnesael M, Gielen E, Boonen S, Vanderschueren D. Skeletal sexual dimorphism: relative contribution of sex steroids, GH-IGF1, and mechanical loading. *J Endocrinol.* 2010;207(2):127-34.
2. Richelson LS, Wahner HW, Melton LJ 3rd, Riggs BL. Relative contributions of aging and estrogen deficiency to postmenopausal bone loss. *N Engl J Med.* 1984;311(20):1273-5.
3. Riggs BL. Endocrine causes of age-related bone loss and osteoporosis. *Novartis Found Symp.* 2002;242:247-59; discussion 60-4.
4. Eastell R. Role of oestrogen in the regulation of bone turnover at the menarche. *J Endocrinol.* 2005;185(2):223-34.
5. Khosla S, Amin S, Orwoll E. Osteoporosis in men. *Endocr Rev.* 2008;29(4):441-64.
6. Callewaert F, Boonen S, Vanderschueren D. Sex steroids and the male skeleton: a tale of two hormones. *Trends Endocrinol Metab.* 2010;21(2):89-95.
7. Falahati-Nini A, Riggs BL, Atkinson EJ, O'Fallon WM, Eastell R, Khosla S. Relative contributions of testosterone and estrogen in regulating bone resorption and formation in normal elderly men. *J Clin Invest.* 2000;106(12):1553-60.
8. Smith EP, Boyd J, Frank GR, et al. Estrogen resistance caused by a mutation in the estrogen-receptor gene in a man. *N Engl J Med.* 1994;331(16):1056-61.
9. Price JS, Sugiyama T, Galea GL, Meakin LB, Sunters A, Lanyon LE. Role of endocrine and paracrine factors in the adaptation of bone to mechanical loading. *Curr Osteoporos Rep.* 2011;9(2):76-82.
10. Vico L, Vanacker JM. Sex hormones and their receptors in bone homeostasis: insights from genetically modified mouse models. *Osteoporos Int.* 2010;21(3):365-72.
11. Khosla S. Pathogenesis of age-related bone loss in humans. *J Gerontol A Biol Sci Med Sci.* 2013;68(10):1226-35.
12. Lee KC, Jessop H, Susillo R, Zaman G, Lanyon LE. The adaptive response of bone to mechanical loading in female transgenic mice is deficient in the absence of oestrogen receptor-alpha and -beta. *J Endocrinol.* 2004;182(2):193-201.
13. Vidal O, Lindberg M, Savendahl L, et al. Disproportional body growth in female estrogen receptor-alpha-inactivated mice. *Biochem Biophys Res Commun.* 1999;265(2):569-71.
14. Lindberg MK, Alatalo SL, Halleen JM, Mohan S, Gustafsson JA, Ohlsson C. Estrogen receptor specificity in the regulation of the skeleton in female mice. *J Endocrinol.* 2001;171(2):229-36.
15. Vidal O, Lindberg MK, Hollberg K, et al. Estrogen receptor specificity in the regulation of skeletal growth and maturation in male mice. *Proc Natl Acad Sci USA.* 2000;97(10):5474-9.
16. Parikka V, Peng Z, Hentunen T, et al. Estrogen responsiveness of bone formation in vitro and altered bone phenotype in aged estrogen receptor-alpha-deficient male and female mice. *Eur J Endocrinol.* 2005;162(2):301-14.
17. Almeida M, Iyer S, Martin-Millan M, et al. Estrogen receptor-alpha signaling in osteoblast progenitors stimulates cortical bone accrual. *J Clin Invest.* 2013;123(1):394-404.

18. Maatta JA, Buki KG, Gu G, et al. Inactivation of estrogen receptor alpha in bone-forming cells induces bone loss in female mice. *FASEB J.* 2013;27(2):478–88.
19. Melville KM, Kelly NH, Khan SA, et al. Female mice lacking estrogen receptor-alpha in osteoblasts have compromised bone mass and strength. *J Bone Miner Res.* 2014;29(2):370–9.
20. Windahl SH, Borjesson AE, Farman HH, et al. Estrogen receptor-alpha in osteocytes is important for trabecular bone formation in male mice. *Proc Natl Acad Sci USA.* 2013;110(6):2294–9.
21. Kondoh S, Inoue K, Igarashi K, et al. Estrogen receptor alpha in osteocytes regulates trabecular bone formation in female mice. *Bone.* 2014;60:68–77.
22. Carolina JM, Evans GL, Harris SA, Zhang M, Westerlind KC, Turner RT. The effects of orbital spaceflight on bone histomorphometry and messenger ribonucleic acid levels for bone matrix proteins and skeletal signaling peptides in ovariectomized growing rats. *Endocrinology.* 1997;138(4):1567–76.
23. Jones HH, Priest JD, Hayes WC, Tichenor CC, Nagel DA. Humeral hypertrophy in response to exercise. *J Bone Joint Surg Am.* 1977;59(2):204–8.
24. Turner CH, Akhter MP, Raab DM, Kimmel DB, Recker RR. A noninvasive, in vivo model for studying strain adaptive bone modeling. *Bone.* 1991;12(2):73–9.
25. De Souza RL, Matsuura M, Eckstein F, Rawlinson SC, Lanyon LE, Pitsillides AA. Non-invasive axial loading of mouse tibiae increases cortical bone formation and modifies trabecular organization: a new model to study cortical and cancellous compartments in a single loaded element. *Bone.* 2005;37(6):810–8.
26. Fritton JC, Myers ER, Wright TM, van der Meulen MC. Loading induces site-specific increases in mineral content assessed by microcomputed tomography of the mouse tibia. *Bone.* 2005;36(6):1030–8.
27. Lee KC, Lanyon LE. Mechanical loading influences bone mass through estrogen receptor alpha. *Exerc Sport Sci Rev.* 2004;32(2):64–8.
28. Ehrlich PJ, Noble BS, Jessop HL, Stevens HY, Mosley JR, Lanyon LE. The effect of in vivo mechanical loading on estrogen receptor alpha expression in rat ulnar osteocytes. *J Bone Miner Res.* 2002;17(9):1646–55.
29. Iyer S, Kim H, Ucer SS, et al. ER α signaling in Osterix1 and Prx1 expressing cells, respectively, mediates the anabolic effect of mechanical loading in the murine periosteum and the protective effects of estrogens on endocortical resorption. *J Bone Miner Res.* 2013;28(S1).
30. Clemens TL, Tang H, Maeda S, et al. Analysis of osteocalcin expression in transgenic mice reveals a species difference in vitamin D regulation of mouse and human osteocalcin genes. *J Bone Miner Res.* 1997;12(10):1570–6.
31. Zhang M, Xuan S, Bouxsein ML, et al. Osteoblast-specific knockout of the insulin-like growth factor (IGF) receptor gene reveals an essential role of IGF signaling in bone matrix mineralization. *J Biol Chem.* 2002;277(46):44005–12.
32. Feng Y, Manka D, Wagner KU, Khan SA. Estrogen receptor-alpha expression in the mammary epithelium is required for ductal and alveolar morphogenesis in mice. *Proc Natl Acad Sci USA.* 2007;104(37):14718–23.
33. Lynch ME, Main RP, Xu Q, et al. Cancellous bone adaptation to tibial compression is not sex dependent in growing mice. *J Appl Physiol (1985).* 2010;109(3):685–91.
34. Holguin N, Brodt MD, Sanchez ME, Kotiya AA, Silva MJ. Adaptation of tibial structure and strength to axial compression depends on loading history in both C57BL/6 and BALB/c mice. *Calcif Tissue Int.* 2013;93(3):211–21.
35. Rubin CT, Lanyon LE. Dynamic strain similarity in vertebrates; an alternative to allometric limb bone scaling. *J Theor Biol.* 1984;107(2):321–7.
36. Dempster DW, Compston JE, Drezner MK, et al. Standardized nomenclature, symbols, and units for bone histomorphometry: a 2012 update of the report of the ASBMR Histomorphometry Nomenclature Committee. *J Bone Miner Res.* 2013;28(1):2–17.
37. Couse JF, Curtis SW, Washburn TF, et al. Analysis of transcription and estrogen insensitivity in the female mouse after targeted disruption of the estrogen receptor gene. *Mol Endocrinol.* 1995;9(11):1441–54.
38. Fritton JC, Myers ER, Wright TM, van der Meulen MC. Bone mass is preserved and cancellous architecture altered due to cyclic loading of the mouse tibia after orchidectomy. *J Bone Miner Res.* 2008;23(5):663–71.
39. Lindberg MK, Moverare S, Skrtic S, et al. Estrogen receptor (ER)-beta reduces ERalpha-regulated gene transcription, supporting a “ying yang” relationship between ERalpha and ERbeta in mice. *Mol Endocrinol.* 2003;17(2):203–8.
40. Castillo AB, Triplett JW, Pavalko FM, Turner CH. Estrogen receptor-beta regulates mechanical signaling in primary osteoblasts. *Am J Physiol Endocrinol Metab.* 2014;306(8):E937–44.
41. Beamer WG, Donahue LR, Rosen CJ, Baylink DJ. Genetic variability in adult bone density among inbred strains of mice. *Bone.* 1996;18(5):397–403.
42. Wergedal JE, Sheng MH, Ackert-Bicknell CL, Beamer WG, Baylink DJ. Genetic variation in femur extrinsic strength in 29 different inbred strains of mice is dependent on variations in femur cross-sectional geometry and bone density. *Bone.* 2005;36(1):111–22.
43. Lynch ME, Main RP, Xu Q, et al. Tibial compression is anabolic in the adult mouse skeleton despite reduced responsiveness with aging. *Bone.* 2011;49(3):439–46.
44. Wakley GK, Schutte HD Jr, Hannon KS, Turner RT. Androgen treatment prevents loss of cancellous bone in the orchidectomized rat. *J Bone Miner Res.* 1991;6(4):325–30.
45. Riggs BL, Khosla S, Melton LJ 3rd. Sex steroids and the construction and conservation of the adult skeleton. *Endocr Rev.* 2002;23(3):279–302.
46. Turner RT, Colvard DS, Spelsberg TC. Estrogen inhibition of periosteal bone formation in rat long bones: down-regulation of gene expression for bone matrix proteins. *Endocrinology.* 1990;127(3):1346–51.
47. Lee K, Jessop H, Suswillo R, Zaman G, Lanyon L. Endocrinology: bone adaptation requires oestrogen receptor-alpha. *Nature.* 2003;424(6947):389.
48. Saxon LK, Galea G, Meakin L, Price J, Lanyon LE. Estrogen receptors alpha and beta have different gender-dependent effects on the adaptive responses to load bearing in cancellous and cortical bone. *Endocrinology.* 2012;153(5):2254–66.
49. Rubinacci A, Marenzana M, Cavani F, et al. Ovariectomy sensitizes rat cortical bone to whole-body vibration. *Calcif Tissue Int.* 2008;82(4):316–26.
50. McKenzie JA, Bixby EC, Silva MJ. Differential gene expression from microarray analysis distinguishes woven and lamellar bone formation in the rat ulna following mechanical loading. *PLoS One.* 2011;6(12):e29328.
51. Meakin LB, Sugiyama T, Galea GL, Browne WJ, Lanyon LE, Price JS. Male mice housed in groups engage in frequent fighting and show a lower response to additional bone loading than females or individually housed males that do not fight. *Bone.* 2013;54(1):113–7.
52. Xiong J, Onal M, Jilka RL, Weinstein RS, Manolagas SC, O’Brien CA. Matrix-embedded cells control osteoclast formation. *Nat Med.* 2011;17(10):1235–41.